Authigenic iron oxyhydroxide rims attenuate deleterious element fluxes during sulphide oxidation in historical gold mine tailings

Steve Jason Chingwaru[1*], Bjorn Von der Heyden[1] and Margreth Tadie[2]

1. Department of Earth Sciences, Stellenbosch University, Private Bag X1, Stellenbosch Matieland, 7602, South Africa
2. Department of Chemical Engineering, Stellenbosch University, Private Bag X1, Matieland, Stellenbosch 7602 South Africa

Supplementary material

Site Description

The Klerksdorp Goldfield (Figure S1a) is one of the major goldfields of the Witwatersrand Basin located on the Kaapvaal craton, South Africa. Gold was first mined at the Klerksdorp goldfields in 1952, and in excess of 5857 tons of gold with additional quantities of uranium have since been extracted from the gold-bearing Vaal Reef (Pienaar *et al.*, 2015; Handley, 2023). The Vaal Reef is an oligomictic conglomerate economic horizon consisting of quartz pebbles associated with heavy detrital minerals such as chromite, rutile, pyrite, uraninite and magnetite. Gold production at the twelve mines in the Klerksdorp Goldfield has accumulated over 600 million tons of historic mine tailings material covering about 900 ha of land (Handley, 2023).

Sample collection and preparation

The primary sample suite for this study was collected from the Vaal Surface Operations tailings storage facilities (TSF), located approximately 8 km south of Klerksdorp town centre and 2.3 km north of the Vaal River (Figure S1b). A total of ~20 kg of material was obtained from spatially discrete drill holes extending to a depth of 10 meters below surface within the TSF. The TSF contains processed material from the Village Main Reef (VMR) Mine and Gold Plant (Figure S1b).

To ensure representativity across the tailings facility, samples from drill holes in close proximity were composited (red dashed line, Figure S1b). Homogenization was achieved through sample preparation techniques involving quarter cone splitting, riffling, and rotary splitting prior to micro-analysis.

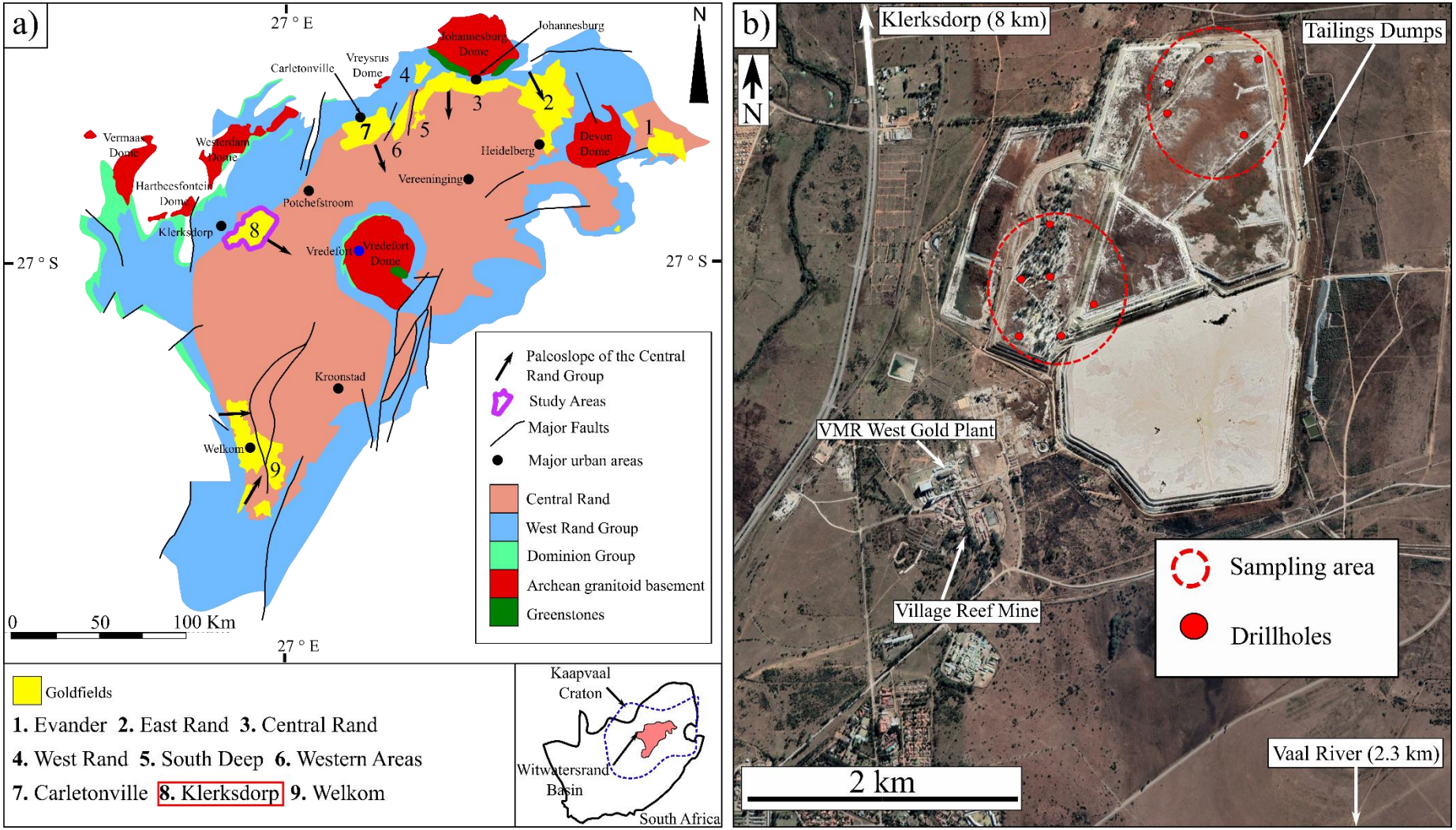

Figure S1: A geological map that shows the Witwatersrand Basin, Dominion Group, Archean granitoids and greenstones. The map also shows the location of the Goldfields with the Klerksdorp Goldfields study area highlighted. **b)** An overhead image of the Klerksdorp tailings dump where sample material was acquired. The red dotted circles are the area of the tailings dump where the sample material was acquired.

Bulk chemistry analysis

The bulk tailings sample material underwent chemical analysis at the Central Analytical Facility (CAF) at Stellenbosch University. This analysis involved aqua regia digestion to determine the bulk concentrations of heavy metals, including As, Cu, Fe, Ni, Zn, Au and Pb. Two dry aliquots of 1 g tailings sample material (duplicated for accuracy), along with a blank sample, underwent microwave-assisted digestion with aqua regia. This digestion process consisted of an acid mixture (3:1), comprising 6 ml of nitric acid (approximately 65% concentration) and 2 ml of hydrochloric acid (approximately 35 % concentration). The samples were digested using a MARS microwave operating at 1600 W power and maintained at 60°C for 6 hours to ensure complete breakdown of aqua regia-digestible minerals. After cooling, the solution was diluted with distilled water to reach a final volume of 50 ml. Inductively coupled plasma mass spectrometry (ICP-MS) measurements were conducted on an Agilent 7900 ICPMS, utilizing the following conditions: 1600 W power level, argon as the carrier gas at 0.83 L/min, make-up gas pumped at 0.15 L/min, and helium and hydrogen flow rates at 5-6 ml/min. The analysis was calibrated against certified reference materials WQB-1 and PTM-1a

Microscopy analysis

The bulk and heavy mineral fraction mounts underwent initial evaluation using reflected light optical microscopy. Optical microscopy was employed for identifying sulphide grains, selecting grains, and observing the weathering characteristics of the sulphide grains. Bulk sample material was mounted in epoxy resin, polished and coated in carbon. The bulk mount sample then underwent mineralogy analysis of the sample was determined through automated electron microscopy using quantitative evaluation of materials by scanning electron microscopy (QEMSCAN) at the University of Cape Town. The QEMSCAN was equipped with a Bruker EDS detector operating at a 20 kV accelerating voltage and 10 nA beam current, using the particle mineral analysis (PMA) function at 425X magnification and a 3 µm pixel size.

The Zeiss EVO MA15VP Scanning Electron Microscopy (SEM) equipped with an Oxford Instruments Wave Dispersive X-ray Spectrometer (WDS) and Oxford INCA software, was employed to determine the element concentrations within the pyrite and the iron oxyhydroxide rims. The SEM is located at CAF and was operating at beam conditions: 20 kV accelerating voltage, 1.0A probe current, an 8.5 mm working distance, a specimen current of − 20.00nA, with a 60 s counting time for the WDS detector.

In-situ ablation analyses

Measurements of heavy metals including Co, Ni, Cu, Zn, As, Au and Pb were conducted using LA ICP-MS at the CAF. Sulphide grains with oxidation rims measuring a minimum of 10 µm in width were selected for in-situ ablation analysis from the heavy mineral sample mounts, resulting in a total of 111 ablation spots in

the pyrite and adjacent iron oxyhydroxide rim. Additionally, ablation was performed on 23 other sulphide minerals to aid in mass balance calculations.

The instruments utilized in this study consisted of a Resolution 193nm Excimer laser from Applied Spectra, coupled with an Agilent 7700 Q ICP-MS, which recorded the concentrations of the heavy metals. Conditions during ablation included a pure helium (He) atmosphere at a flow rate of 0.4 L/min, laser energy set at 2.8 J/cm², a frequency of 7 Hz, and, before transportation to the ICP-MS, the ablated material was mixed with argon (Ar, 0.95 L/min) and nitrogen (N, 0.003 L/min). In-situ ablation was performed using a spot size of 20 µm on the unaltered pyrite core and 10 µm for the oxidized pyrite rim. Ablation time was set at 45 seconds with a background acquisition time of 15 seconds. Quality control and calibration were achieved using standards NIST 610, Po 725 and MASS-1. The resulting data were processed using LADR version 1.1.08 software from Norris Scientific (Norris & Danyushevsky, 2018). To correct for variations in ablation yields between grains and standards, an internal standard element with a known concentration was employed (Longerich *et al.*,1997).

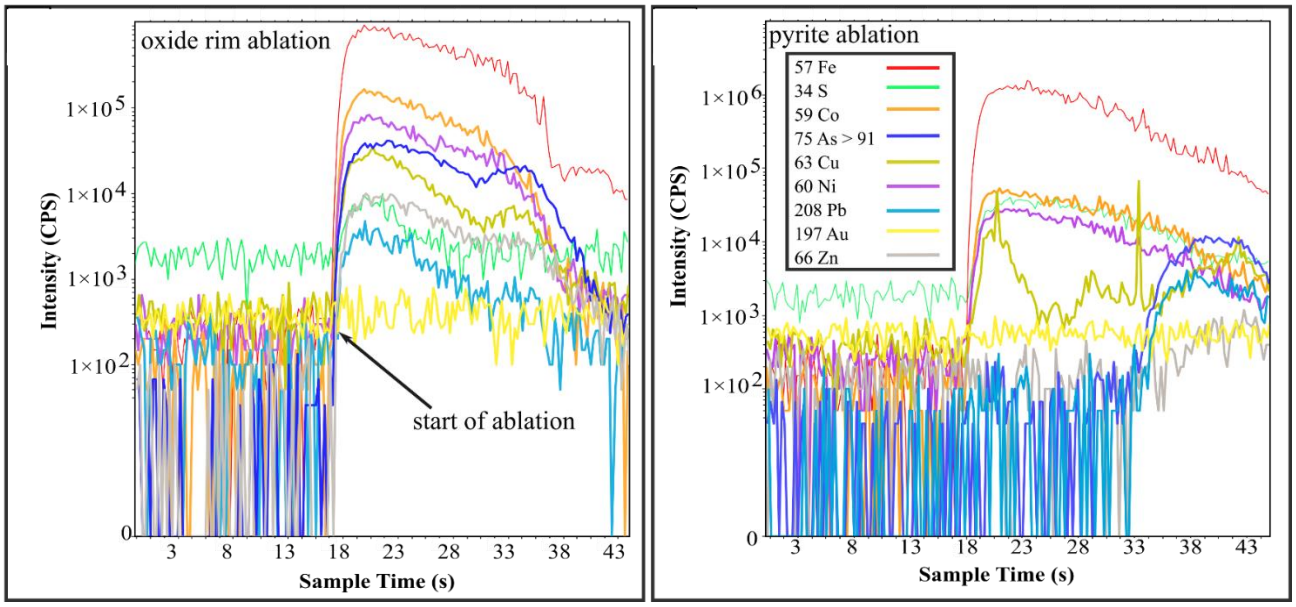

Figure S2: The corresponding LA ICP-MS time-resolved spectra graphs from the in situ ablation of (**Left**) the iron oxyhydroxide alteration product and (**Right**) pyrite

Mass balance, leaching coefficient and D-value calculations

Leaching Coefficient calculations

To determine the heavy metal mobility from the sulphide to the oxidation alteration product a (*LE*) leaching coefficient was calculated using the following equation (Diao & Wen, 1999; Lu *et al.*, 2005).

$$LE = \frac{C_{py} - C_{ox}}{C_{py}} \times 100, \quad (1)$$

The LE was calculated using the following assumptions: 1) The total mass of the iron remains constant during pyrite oxidation, considering iron is a major element of pyrite and immobile during weathering (Lu *et al.*, 2005). 2) Assuming the alteration product from pyrite oxidation in the sample material forms an iron hydroxide based on the oxidation reaction formula (Dos Santos *et al.*, 2016) :

$$4FeS_2 + 15O_2 + 14H_2O \rightarrow 4Fe(OH)_3 + 8H_2SO_4 \quad (2)$$

The LA ICP-MS data for the iron oxyhydroxide rims were normalized during the quantification set-up in the data reduction software LADR (Laser Ablation Data Reduction). The normalisation step converted the internal standard ^{57}Fe signal into concentration values relevant to $Fe(OH)_3$ stoichiometry which was used as the proxy speciation for the Fe (oxy-)hydroxide rims. In low-temperature geochemical systems, the speciation of the ambient iron (oxy-)hydroxides is commonly quite complex, comprising finely-intergrown mixtures of Fe oxides (e.g., hematite), Fe oxy-hydroxides (e.g., goethite, lepidocrocite) and poorly-crystalline phases (e.g., ferrihydrite) (Cornell & Schwertmann, 2003; von der Heyden & Roychoudhury, 2015). The normalisations applied during the quantification step in LADR are shown in Figure S2.

For the LE calculation given by equation 1, C_{py} represents the average concentration of the metal in the unaltered pyrite core, and C_{ox} represents the average concentration of the metal within the oxide alteration rims. These concentrations were determined through LA-ICP-MS analysis. A positive LE value indicates the leaching of the metal into the TSF system, while a negative LE denotes the enrichment of the metal in the local oxidation rims. The estimation of LE is based on the assumption that the total mass of the metals remains constant during the weathering of pyrite.

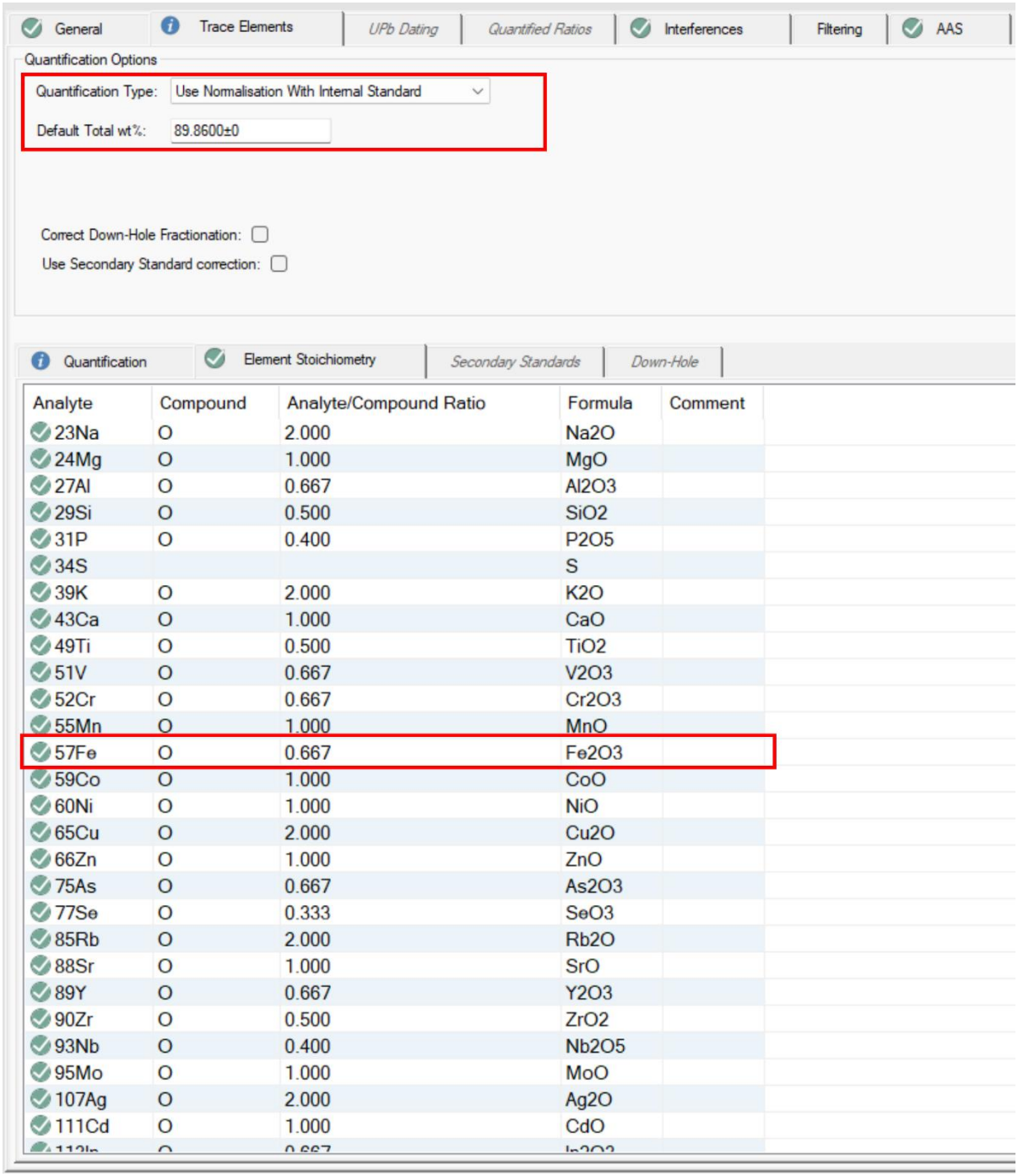

Figure S3: An example of a normalized quantification setup in LADR for iron oxyhydroxide. Note the red rectangles highlight the data reduction was normalized to Fe_2O_3 (89.86 wt.%) against an internal standard of ^{57}Fe to best replicate iron oxyhydroxide in nature.

Mass balance calculations

Mass balance calculations were performed to determine the total metal percentage distribution in each phase within the tailings sample material. These calculations were done using the formula (Chingwaru *et al.*, 2023):

$$\text{Phase deportment } (\%) = \frac{m_{phase}}{m_{total}} \times 100, \quad (3)$$

Where m_{total} represents the total mass of the element within the tailings sample material, determined using the mass of the sample (m_{sample}) and the total metal concentration (c_{total}) determined through aqua regia and ICP-MS analysis. The formula for m_{total} is as follows:

$$m_{total} = m_{sample} \times c_{total} \quad (4)$$

In formula (3), m_{phase} stands for the mass of the metal hosted within a specific phase within the tailings. m_{phase} is determined using the percentage of the mineral phase (% phase) determined by QEMSCAN, the total sample mass (m_{sample}), and the average metal concentration within that specific mineral phase (c_p) measured using LA ICP-MS. The formula to determine m_{phase} is as follows:

$$m_{phase} = (\%\ phase \times m_{sample}) \times c_p \quad (5)$$

The deportment labelled that is referred to as discrete fraction (unaccounted fraction) is deportment that is from elemental phases that were not measured by ablation analysis. This was determined by subtracting the total elemental mass (m_{total}) from the sum of all the m_{phases} .

Mass balance calculations example

An example will be calculating the total deportment of arsenic in pyrite.

The total mass of As in the sample is calculated using Equation **4**. $m_{total} = m_{sample} \times c_{total}$

0.0004777 g × 36.44 ppm = 0.017 g of As is within the sample material.

The mass of As hosted in pyrite is calculated using Equation **5**. $m_{phase} = (\%\ phase \times m_{sample}) \times c_p$

(1.31 % × 0.0004777) × 713.18 ppm = 4.46×10^{-3} g of As is hosted within pyrite

The total deportment is then calculated using Equation **3.** $\text{Phase deportment } (\%) = \frac{m_{phase}}{m_{total}} \times 100$,

$\frac{4.46 \times 10^{-3}\ g}{0.017\ g} \times 100 = 26$ % of total As is distributed within pyrite

Bulk Mineralogy

Table S1: Showing the bulk mineralogical make-up of the tailings sample material determined by QEMSCAN analysis (duplicate analyses). Other sulphides* refer to arsenopyrite, sphalerite, pyrrhotite and galena. Other* refers to accessory minerals such as barite etc.

Mineral	**Calculated modal proportion (wt.%)**
Quartz	62.08
Feldspar	6.21
Pyroxene	0.42
Amphibole	0.10
Chlorite	9.58
Kaolinite	0.98

Pyrophyllite	6.25
Mica	10.47
Zircon	0.07
Total Silicates	**96.16**
Pyrite	1.31
Chalcopyrite	0.16
Other sulphides*	0.03
Total Sulphides	**1.50**
Fe oxide/hydroxide	1.01
Rutile	0.83
Chromite	0.07
Total Oxides	**2.11**
Apatite	0.01
Carbonates	0.01
Total Phosphates & Carbonates	**0.02**
Others*	0.41
Total	**100**

Figure S4: Boxplots showing the weight percentages of elements in the iron oxyhydroxide rims, as determined by SEM analysis.

References

Chingwaru, S.J., Heyden, B. Von Der & Tadie, M. 2023. An underexploited invisible gold resource in the Archean sulphides of the Witwatersrand tailings dumps. *Scientific Reports*. 13(3086):1–10. DOI: 10.1038/s41598-023-30219-5.

Cornell, R.M. & Schwertmann, U. 2003. *The Iron Oxides : Structure, Properties, Reactions, Occurences and Uses*. vol. 664. Wiley. DOI: 10.1002/3527602097.

Diao, G. & Wen, Q. 1999. Mobility sequence of chemical elements during loess weathering-pedogenesis, Weinan, Shaanxi Province, China. *Chinese Journal of Geochemistry*. 18:327–332.

Handley, M. 2023. Where is all the gold? *Journal of the Southern African Institute of Mining and Metallurgy*. 123(4):175–192. DOI: 10.17159/2411-9717/1902/2023.

von der Heyden, B.P. & Roychoudhury, A.N. 2015. A review of colloidal iron partitioning and distribution in the open ocean. *Marine Chemistry*. 177:9–19. DOI: 10.1016/j.marchem.2015.05.010.

Longerich, H.P., Jackson, S.E. & Gunther, D. 1997. Laser ablation inductively coupled plasma mass spectrometric transient signal data acquisition and analyte concentration calculation. *Journal of Analytical Atomic Spectrometry*. 12(3):391.

Lu, L., Wang, R., Chen, F., Xue, J., Zhang, P. & Lu, J. 2005. Element mobility during pyrite weathering: Implications for acid and heavy metal pollution at mining-impacted sites. *Environmental Geology*. 49(1):82–89. DOI: 10.1007/s00254-005-0061-8.

Norris, A. & Danyushevsky, L. 2018. Towards Estimating the Complete Uncertainty Budget of Quantified Results Measured by LA-ICP-MS. *Goldschmidt: Boston, MA, USA.*

Pienaar, D., Guy, B.M., Hofmann, A. & Viljoen, K.S. 2015. A geometallurgical characterization of the Vaal Reef A-facies at the Moab Khotsong mine, Klerksdorp goldfield, South Africa. *South African Journal of Geology*. 118(4):455–472. DOI: 10.2113/gssajg.118.4.455.

Dos Santos, E.C., De Mendonça Silva, J.C. & Duarte, H.A. 2016. Pyrite Oxidation Mechanism by Oxygen in Aqueous Medium. *Journal of Physical Chemistry C*. 120(5):2760–2768. DOI: 10.1021/acs.jpcc.5b10949.